



RESEARCH ARTICLE
DOI: 10.47750/jptcp.2023.1074

The added value of diffusion weighted MRI over standard dynamic liver MRI in characterization of focal liver lesions

Hayder Suhail Najm Alareer^{1,2}, Hayder Jasim Taher^{1,3*}, Hussein Abed Dakhil², Ayoob Dinar Abdullah⁴, Ahmed Mohamedbaqer Easa², Raad Ajeel Bustan²

¹Department of Technology of Radiology and Radiotherapy, Tehran University of Medical Sciences, International Campus, Tehran, Iran.

²Department of Radiological, Collage of Health & Medical Technology, Al-Ayen University, Thi-Qar, Iraq.

³Department of Radiology, Hilla University College, Hilla, Iraq.

⁴Radiology Technology department Al-Manara college for medical sciences, Missan, Iraq.

***Corresponding author:** Hayder Suhail Najm Alareer, Technology of Radiology and Radiotherapy Dept, Tehran University of Medical Sciences, International Campus, Tehran, Iran, Email: hayder.suhail85.hs@gmail.com

Submitted: 11 November 2022; Accepted: 22 December 2022; Published: 19 January 2023

ABSTRACT

Background: The study aims to assay the value of diffusion-weighted MR imaging over conventional dynamic liver MRI in the characterization and distinguishing of localized benign and malignant alterations in liver mass.

Methods: All liver MRI scans taken at Imam Khomeini Hospital Imaging Center from November 2018 to October 2021 were studied. Demographic information of patients was recorded. One hundred and forty patients with 221 liver lesions and focal liver tumors were evaluated using TSE T2WI, GE T1WI, 3-T MRI tests. Dynamic imaging was performed using T1 THRIVE. The results were compared with histopathology, laboratory and other previous radiological results (US &/or MSCT) performed on all patients. All collected data were analysis with SPSS VER 18 software.

Results: Among the 140 individuals studied, 221 liver lesions were identified. The average age of the patients was 51.1 ± 12.4 years, of all the patients investigated in the present study, there were 68 men and 72 women. The lesions were cysts (24), hemangiomas (81), FNH (9), adenomas, (10), peliosis hepatis (4), HCC (33), metastasis (58), cholangiocarcinoma (1), and Epithelioid hemangioendothelioma (1). means of ADC at the Cutoff point ≤ 1000 corresponded to sensitivity, specificity, positive and negative predictive value, and accuracy (100 %, 96 %, 95 %, 100, and 98 %). the diagnostic indicators of dynamic research obtained as follows specificity, sensitivity, negative and positive predictive value, and accuracy found accordingly (% , 97 %, 96 p%, 98 %, and 98 %).

Conclusion: We expect to minimize the number of biopsies and costs by using DWI over dynamic MRI to identify the features of liver lesions (malignant or benign). Using DWI on dynamic MRI results to identify liver malignant or benign lesions is expected to minimize the number and the costs of biopsies.

Keywords: *Magnetic Resonance Imaging, diffusion-weighted MRI, focal liver lesions*

1. INTRODUCTION

Numerous benign, malignant, and localized metastatic lesions are assumed to occur in the liver (1). To treat patients with liver neoplasms, including hepatocellular carcinoma (HCC) and metastases, requires precise identification and characterization of focal liver lesions (FLLs). Because patients with less resectable metastatic lesions can benefit from resection therapy. Therefore, the number and size of lesions may affect treatment. In more severe conditions of the disease, systemic chemotherapy, radiofrequency ablation or trans-arterial chemoembolization should be performed (1). MR imaging has turned into a vital imaging modality for evaluating hepatic nodules, and it is superior to all other imaging modalities for precise differentiation between and malignant benign hepatic masses (2). The interaction of water with the cell membrane and macromolecules as well as microcirculation determines the free diffusion rate in biological tissues. diffusion-weighted imaging (DWI) an MR technique provides the possibility of investigating tissue microstructure based on variable degrees of water diffusion and microperfusion. DWI may considerably decrease the intravenous contrast medium delivery requirement to investigate malignancies. After adding strong bipolar pulses to spin or gradient echo sequences with different b-values, DWI can be obtained (3).

Single shot echo planar echo imaging sequence (SS SE EPI) is the most widely used sequence for liver DWI. Also, Apparent Diffusion Coefficient (ADC) is usually used as a measure of diffusion instead of diffusion coefficient in biological systems. Studies have shown that DWI has the potential to characterize focal liver lesions (eg, distinguish between hemangioma and hepatocellular carcinoma [HCC]) based on ADC values (4). Improved image quality and detection of focal liver lesions using RT DWI has been demonstrated in the past in several studies (5,6). A reduction in ADC calculation errors occurs with higher SNR, longer TR, and multiple b-values obtained with RT sequences (7).

This research aimed to assess the increased utility of DWI over conventional dynamic liver MRI in the description of localized liver lesions. In addition, we intended to examine the optimal cutoff value for distinguishing benign from malignant liver lesions.

2. MATERIALS AND METHODS

2.1. Study population

We examined all liver MRI examinations conducted at Imam Khomeini hospital from November 2018 to October 2021.

They were in Imam Khomeini hospital. The protocols for this research were confirmed by the ethics committee of the International Campus of Tehran University of Medical Sciences (IR.TUMS.SPH.REC.1396.2297).

After an explanation of the study's methodology, written consent was acquired from each participant. The researchers recruited patients with localized hepatic lesions diagnosed by the US and/or MSCT. Lesions less than 1 cm, unstable medical condition, and contraindications to MR imaging (claustrophobia, pacemaker patients), along with a history of tumoral hepatic lesion treatment (radiotherapy or chemotherapy), immunodeficiency history, were eliminated from the study. If the patients meet the research's inclusion and exclusion requirements, they will all be progressively included in the trial. Laboratory results and patient demographic information were documented. All subjects had an abdominal MRI with diffusion-weighted imaging and pre-and post-contrast studies. The outcomes have been compared with the histopathology, laboratory, and other prior radiological (US&/or MSCT) results performed on all patient populations.

2.2. Liver MRI imaging protocol

Liver imaging was performed using MRI with a power gradient of 45 mT/m on a high field (3 Tesla) magnet unit (Siemens MAGNETOM TRIO) with a phased array coil. MRI protocols include the following:

T1 weighted (T1W) images have the following specifications: repetition time TR=10 msec, echo time TE=4.58 msec, matrix 179x320, slice thickness 7-8 mm, slice gap 1-2 mm, and FOV 355 mm.

TR = 2000 msec, TE = 221 msec, matrix 320 x 240, slice thickness 6.0 mm, slice gap 1-2 mm, and FOV 366 for T2 weighted (T2W) images (single shot free breathing).

The parameters used in the T2 SPAIR fat suppression sequence: TE=80msec, TR≥4000msec, slice thickness 6.0mm, matrix 204x384, slice gap 1-

2mm, and FOV 365.

Out phase, and in phase gradient echo sequence (Dual/FFE): TE = 4.6 ms for (in phase), and 2.3 ms (out phase), TR = 164 ms, slice thickness = 6.0 mm, matrix = 143 x 240, slice gap = 0 mm, and FOV = 360.

An active investigation was conducted following a bolus injection of Gd-DTPA at a rate of 0.1mmol/kg body weight and 20ml of sterile 0.9 percent saline solution into the antecubital vein. The saline solution injection and the contrast media injection were carried out by hand. Three phases of dynamic imaging were carried out utilizing the T1 THRIVE (High-Resolution Isotropic Volume Examination) method: the arterial phase (16–20 s), the Porto-venous phase (45–60 s), and the delayed equilibrium phase (3-5 s) after the use of the contrast agent. To maximize sensitivity to cellular packing, respiratory-triggered fat-suppressed single-shot echo-planar DW imaging was carried out in the transverse plane with tri-directional diffusion gradients utilizing b values (50, 500, &800) sec/mm². Parallel imaging using generalized auto-calibrating partially parallel acquisition (GRAPPA) with a two-fold acceleration factor was used to enhance image quality. In addition, the following parameters have been used: repetition time (TR) = 4400 msec, echo time (TE) = 76 msec, number of excitations (NEX) = 3, matrix 256x256, slice thickness 6.0 mm, slice gap 1-2 mm, scan time 3–4 min, and a field of view as small as possible with a 52 percent rectangular field of view.

2.3. Imaging Analysis

The shape, size, margin, signal characteristics (T1W&T2W), the pattern of enhancement in dynamic imaging, and the number and location of discovered FLLs were recorded for every lesion. After then, a tentative diagnosis was made accessible. Second, we evaluated the enhanced diagnostic value of the diffusion images in identifying and characterizing FLLs by analyzing the diffusion images.

On DWI, limited diffusion was evaluated if a lesion displayed higher signals relative to the normal liver parenchyma on rising b-value images. ADC values were utilized for the overall radiological identification and characterization of FLLs. The mean ADC of every identified FLLs is calculated by defining a region of interest (ROI) encompassing the entire lesion and the high & low sections of the lesion (Figure 1). The ADC was measured twice, and the average of the two observations was calculated. Regions of interest have been copied and pasted from DW photos to ADC maps; quantitative analysis of ADC calculations depending on a threshold of 1.210-3mm²/s, to certify that similar areas were assessed. Below that point, all lesions are regarded as malignant lesions. Hemangiomas and cysts display the T2 shine-through effect, characterized by a bright signal on both diffusion images and the ADC map. For FLL identification and characterization, two independent observers examined DW (b values of 50, 500, and 1000 sec/mm²) and T2-weighted images. The two observers' consensus analysis of DW, T2-weighted, and dynamic contrast material-enhanced images, pathologic information, and follow-up imaging findings resulted in the reference standard for diagnosis. For FLLs found by consensus review, the ADC was calculated.

2.4. Statistical analysis

All collected data were entered into SPSS VER 18 software. To compare quantitative variables, the independent sample t-test was utilized. A binary logistic regression model was used to compare DW and T2-weighted images for FLL identification and characterization. By measuring the area under the ROC curve, the accuracy of each MR method (ADC and conventional dynamic liver MRI) was assessed (AUC). The importance of the variations between ROC curves was evaluated. P values below 0.001 were regarded as significant.

3. RESULTS

This research comprised 140 individuals (72 women and 68 men) with 221 liver lesions. The average patient age (18–86) was 51.1±12.4 years. There was no statistically significant difference between malignant and benign lesions in terms of gender (p-value: 0.14). 42.1% (93 case) of lesions were malignant and 57.9% (128 case) were benign. The precise number of every kind of lesion display in table 1. Follow-up revealed the ultimate diagnosis in 48 percent of cases (106 lesions), and biopsy revealed it in 52 percent of cases (115 lesions). 3 lesions were typical HCC and did not need a biopsy for diagnosis; therefore, 96.8% malignant lesions, were proven by biopsy. In comparison, 80% of benign lesions, were proven by follow-up, and just 19.5% were proven by biopsy.

DCE MRI was extremely useful for distinguishing benign from malignant lesions (p value< 0.001). Lesions without enhancement were usually benign. In 79 benign lesions with the following criteria were observed: the existence of arterial peripheral nodular enhancement with delayed centripetal fill-in entirely consistent with the type of the lesion, and washout with central scar enhancement (as mentioned in nine patients). The presence of enhanced venous rims, and the existence of arterial input and venous output was one of the criteria to diagnose a malignant lesion. (Table 2). We discovered the ADC value to be accurate for distinguishing benign from malignant lesions. ADC hyperintensity was seen in 124 of 128 benign lesions, while all malignant lesions had hypointense ADC (restricted diffusion). To differentiate between benign and malignant hepatic lesions a cut-off point of ADC ratio ≤ 0.87 was established as the optimum criterion for differentiating malignant from benign hepatic lesions and the ADC value demonstrated sensitivity, specificity, and accuracy of 100%, 97%, and 98%.

TABLE 1. lists the pathological categories for the hepatic focal lesions examined in the investigation.

lesion type	Frequency	Percent
Cyst	24	10.9
Hemangioma	81	36.7
FNH	9	4.1
Adenoma	10	4.5
Metastasis	58	26.2
HCC	33	14.9
Cholangiocarcinoma	1	.5
Epithelioid Hemangioendothelioma	1	.5
Peliosis hepatis	4	1.8
Total	221	100.0

TABLE 2: dynamic contrast-enhanced MRI characterizes different hepatic lesions: P-Value<0.001

Different hepatic lesions	Final result		Total
	benign	malignant	
PNE+ centripetal fill-in	81 100.0%	0 .0%	81 100.0%
Non-enhancement	24 100.0%	0 .0%	24 100.0%
Rim+ centripetal fill-in	0 .0%	27 100.0%	27 100.0%
Heterogeneous	3 100.0%	0 .0%	3 100.0%
Rim enhancement	0 .0%	29 100.0%	29 100.0%
Iso+ arterial wash-in	0 .0%	2 100.0%	2 100.0%
Homogeneous with isointense	10 100.0%	0 .0%	10 100.0%
Heterogeneous enhancement	0 .0%	1 100.0%	1 100.0%
Wash-in+ wash-out +capsular enhancement	0 .0%	21 100.0%	21 100.0%
Wash-in and wash-out	1 7.1%	13 92.9%	14 100.0%
Wash-in and iso scar enhancement	9 100.0%	0 .0%	9 100.0%
Total	128 57.9%	93 42.1%	221 100.0%

TABLE 3. describes the focal liver lesions in the 140 individuals who were the subject of the study

Type of lesion	no	T1W I	T2WI	IN/OUT phase	DWI		dynamic
					DWI	ADC	
Cyst	2 4	↓	↑ ↑	no fat	↑	↑	no enhancement +no
Hemangioma	8 1	↓	↑ ↑	no fat	↑	↑	PNE+ centripetal fill-in
FNH	9	Iso	mild to moderate hyperintense	fat	↓	↑	Enhancement except scar +enhancement with scar
Adenoma	1 0	Iso	Iso	fat	↓	↑	homogeneous enhancement+ iso
peliosis hepatis	4	↓	mild to moderate hyperintense	no fat	↑	↓	no enhancement+ heterogeneous enhancement
Metastasis	5 8	↓	mild to moderate hyperintense	no fat	↑	↓	Rim+ rim-+ centripetal fill in
HCC	3 3	↓	mild to moderate hyperintense	fat	↑	↓	wash in + washout+ capsular enhancement
Cholangiocarcinoma	1	↓	mild to moderate hyperintense	no fat	↑	↓	Rim+ gradually fill in
Epithelioid Hemangioendotheloma	1	↓	heterogeneous mild to moderate	no fat	↑	↓	heterogeneous enhancement+ heterogeneous enhancement
Total	2 2 1						

Compared to the adjacent normal liver, arrows denote signal intensities that

are either hyperintense ("up" arrow) or hypointense ("down" arrow). Double-up arrows denote extreme intensity. Iso =isointense. SI =signal intensity.

TABLE 4. Descriptive: the number of lesions, the amount of ADC, and the P-Value

Type of lesion	No	ADCPMEAN	ADCSD	ADCPRATIO	ADCWMEAN	ADCWSD	ADCWRATIO	P-Value
Cyst	24	2.8	231.82	1.4	2.6	368.03	1.3	<0.001
Hemangioma	81	1.9	160.67	1.04	1.8	246.69	0.98	<0.001
FNH	9	1.2	183.23	0.65	1.2	209.005	0.67	<0.001
Adenoma	10	1.4	191.40	0.73	1.4	232.82	0.74	<0.001
Metastasis	58	0.8	124.104	0.42	0.9	232.91	0.55	<0.001
HCC	33	0.85	168.83	0.41	0.96	226.69	0.46	<0.001
Cholangiocarcinoma	1	1.03	101.82	0.51	1.09	182.02	0.53	<0.001
Epithelioid Hemangioendothelioma	1	1.02	147.37	0.38	1.1	263.17	0.42	<0.001
Peliosis hepatis	4	0.9	184.03	0.44	0.9	276.85	0.47	<0.001
Total	221							

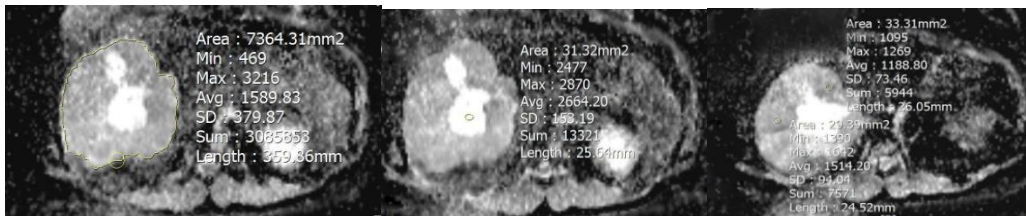


FIGURE 1. drawing a region of interest (ROI)

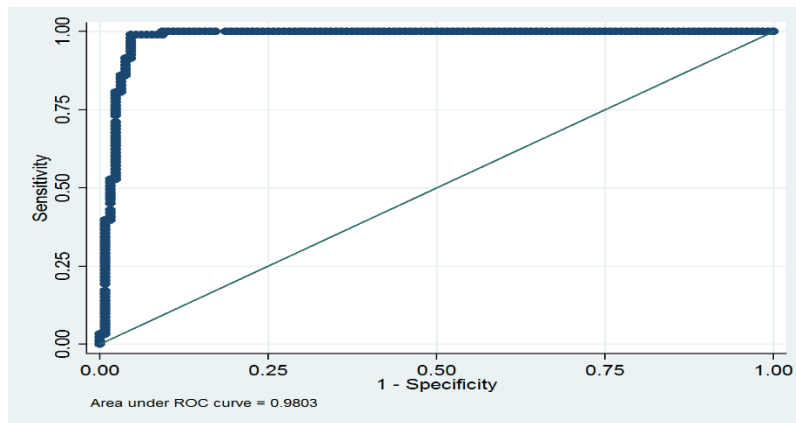


FIGURE 2. ROC curve of ADC value

5. DISCUSSION

The aim of our study was to assess the use of ADC values for distinguishing benign from malignant localized liver lesions. We discovered that DWI and dynamic contrast-enhanced liver MRI are similar for such an objective. Multiple dynamic characteristics were significantly diagnostic for distinguishing benign from malignant lesions. Hemangioma diagnosis was usually made by observing arterial peripheral nodular enhancement with a delayed centripetal fill-in pattern. Another sign of benignity was the existence of washout with central scar enhancement. On the other hand, malignancy was consistent with venous rim enhancement. The occurrence of arterial wash-in and venous wash-out strongly suggested a malignant lesion; nonetheless, there was an instance of overlap.

Regarding the quantitative examination of ADC values, metastases and HCCs had the lowest ADCs, while cysts and hemangiomas had the greatest. The ADC mean total, part, and the ratio of benign and malignant lesions differed significantly. There was no change in ADC values between different benign and malignant lesions in any sequence.

In this investigation, there were 24 cystic lesions on 15 individuals. The common lesion on an MRI seems to have a geographic or rounded form, is strongly described, hypointense on T1WI images, and is noticeably prominent on T2WI images with no signal reduction throughout the in/out phase. Cysts do not seem amplified in any dynamic pattern on contrast-enhanced images. Cysts appear hyperintense on diffusion-weighted imaging, not because of limitation but instead T2 shine-through. This is because cysts have an enlarged extracellular space compared to normal tissue. Consequently, these lesions are characterized by free diffusion and increased ADC values. ADCs of cysts are the largest of all focal liver lesions, most likely because of the

vascular space and, consequently, blood flow or perfusion inside the cyst Goshima et al. The diagnosis of the 15 instances of cyst presented in the current investigation was uncomplicated based on existing literature about MRI signal characteristics, contrast enhancement patterns, and diffusion research criteria.

The most frequent benign hepatic tumor is a hemangioma, a solid, cavernous liver tumor (8,9). This research included 49 individuals with 81 lesions. In large hemangioma, six individuals have scars, whereas one has a sclerosing hemangioma (with cirrhosis). The common lesion on an MRI has a spherical or geographic shape, is hypointense on T1WI, does not show a signal decline during the In/Out phase (meaning there is no fat), and is significantly elevated on T2WI. Hemangiomas exhibit early peripheral nodular enhancement (PNE) and progressive centripetal enhancement on successive images taken using contrast-enhanced imaging. This is consistent with results of Bozgeyik et al. study (10). They showed that the peripheral enhancement on the initial phase pictures is often nodular and discontinuous, with centripetal filling during the portal venous phase and virtually filled with contrast on the delayed images. Hemangiomas appear hyperintense on diffusion-weighted imaging due to T2 shine-through rather than limitation. This is because enlargement of the extracellular space compared to normal tissue characterizes hemangiomas.

Consequently, these lesions are characterized by free diffusion and increased ADC values. Goshima et al. (2008) suggested that Hemangiomas have ADCs higher than solid lesions yet less than cysts, most likely due to the vascular space and consequent blood flow or perfusion inside hemangiomas. The diagnosis of the two instances of hemangioma presented in the current investigation was uncomplicated based on existing literature about the MRI signal, contrast enhancement pattern, and diffusion investigation parameters.

FNHs are benign tumors that are considered to develop in response to congenital vascular abnormalities that cause hyperplasia in this investigation, nine lesions with FNHs on MRI that were isointense on T1WI and mild to moderately hyperintense with a scar on T2WI images showed minimal signal loss throughout the in/out phase. FNHs display enhancement on contrast-enhanced pictures, except for the scar on arterial enhancement, which becomes isointense to the liver's backdrop on portal venous imaging, and augmentation with the scar in the center on equilibrium phases. They might have a central scar, which is generally hypo enhancing in the arterial phase but may show enhancement in the later phases. With rising b-values on DWI, FNH displays a modest increase in signal strength but remains hypo-intense on the ADC map. This is consistent with (11).

Hepatocellular tumors called hepatic adenomas are uncommon and benign (12). The subtype and the presence of bleeding or fat inside the tumor determine their appearance. The research included ten adenoma lesions. On MRI, the tissue is isointense on T1WI, has a substantial signal loss during the In/Out phase due to fat content, and is isointense to hyperintense on T2WI images. On arterial phase contrast-enhanced imaging, the hepatic adenoma looks homogeneous; on portal and equilibrium phase images, it appears iso-enhancing. This is consistent with the findings of Ba-Ssalamah et al study (13). In diffusion-weighted imaging, the signal intensity of the nodule increases somewhat with rising b-values on DWI and is hypointense on ADC maps. This is consistent with the results of Kilickesmez et al. study (14).

Peliosis, an uncommon benign condition defined by the formation of widespread blood-filled cystic spaces (15), may affect the liver. In our study, there were four Peliosis hepatitis lesions, two men (50 percent) and two women (50 percent). Fat is not detected in the In/Out phase of MRI using T1WI, and T2WI pictures are mild to reasonably hyperintense with a partial signal loss on heavy T2WI.

In contrast-enhanced images, the peliosis hepatitis seems heterogeneously elevated in the portal and delayed phases but not enhanced at all in the arterial phase. This is consistent with the findings of Ba-Ssalamah et al. study (2010). Peliosis appears hyperintense on diffusion-weighted imaging (DWI) with rising b-values and hypointense on ADC maps. This is consistent with the results of (16).

In the present study, thirty-two instances of cirrhosis of the liver were discovered. HCC is often hypointense on T1-weighted MR imaging, with a discernible signal loss in the In/out phase owing to the presence of fat; nevertheless, hyperintense lesions or hyperintense regions within hypointense lesions could be observed. The presence of fat, protein, or blood in these hyperintense areas inside the HCC indicates intraregional hemorrhage. HCC is often mild to moderately hyperintense on T2-weighted imaging, albeit well-differentiated lesions that seem to be isointense compared to the liver parenchyma may be visible. Most HCCs display significant enhancement with a quick wash in subsequent phases on arterial phase contrast-enhanced images. On arterial phase dynamic gadolinium-enhanced imaging, most small HCCs display considerable enhancement with a rapid washout at the portal phase and, in a few instances, at the capsule phase. HCCs may present in different ways on diffusion-weighted imaging. Well-differentiated tumors are usually isointense compared to moderately to poorly differentiated tumors, which are more frequently hyperintense and have lower ADC values. This is consistent with Nasu et al.,(17) and would be confirmatory for HCC, particularly when other MRI characteristics of HCC are observed.

Intrahepatic cholangiocarcinoma is the predominant bile duct-derived malignancy of the liver (18). According to the investigation, a single female patient was diagnosed with cholangiocarcinoma. On an MRI, the following characteristics are present:

Hypointensity on T1WI, in/out phase with no signal loss, mild to moderate hyperintensity on T2WI images, and signal loss in heavy T1WI. CCC shows rim enhancement on contrast-enhanced images during the arterial phase and gradually fills in throughout the portal venous and delayed phases. Following (19), intrahepatic cholangiocarcinoma might have restricted diffusion on images having high b values and low ADC values on diffusion-weighted imaging.

One female patient had epithelioid hemangioendothelioma in this investigation. Epithelioid hemangioendothelioma is a rare vascular tumor with a moderate risk for malignancy (20). Numerous nodules in both hepatobiliary lobes are the most common form of (HEHE). Based on its radiologic symptoms, it might be misinterpreted as metastatic carcinoma, a soft tissue vascular tumor of endothelial origin with a clinical history intermediate between benign hemangioma and malignant angiosarcoma. Hypo-intense on T1WI, no fat in the In/Out phase, mild to moderate heterogeneity on T2WI pictures, and a partial signal loss in heavy T2WI were the findings on an MRI scan. The arterial, portal, and equilibrium phases are heterogeneous in contrast-enhanced images. Epithelioid hemangioendothelioma is hyperintense and has low ADC values on diffusion-weighted imaging (21).

The T1 and T2 signal intensities of liver metastases vary; however, they are frequently protracted; consequently, T1-weighted MR images are hypo intense, and the In/out phase is fat. On contrast-enhanced images, they demonstrate delayed enhancement, total signal loss in heavy T2WI, and mild to moderate hyperintensity on T2-weighted images. Often, they exhibit early rim augmentation. Some of the most frequent primary tumors that lead to hypervascular hepatic metastases are islet cell tumors, breast cancer, ovarian cancer, melanoma, thyroid cancer, and carcinoid tumor. The arterial phase of enhancement is when hypervascular metastases are most visible, and delayed pictures reveal the rim to centripetal fill in

(22). In our study, 30 individuals were assessed for 58 metastatic lesions. The main tumors were stomach in four cases, perianal in four cases, colorectal carcinoma in 25 patients, rectal cancer in seven cases, cecum in four cases, cervix in five cases, breast cancer in three cases, neuroendocrine tumor in three cases, and undetermined primary in two cases. Identifying these lesions was uncomplicated concerning the clinical history of original malignancy, typical MRI characteristics, the pattern of contrast enhancement, and diffusion research parameters. According to (23), malignant hepatic tumors, particularly hepatic metastases, have a lower apparent diffusion coefficient than benign nodules.

Hepatic metastases will often exhibit limited diffusion on images with a high b value and low ADC values. On high b value diffusion images, on the other hand, cystic or necrotic metastases will exhibit more signal attenuation and provide larger ADC values (24,25). There are some drawbacks to using respiratory-triggered images. ADC results may be somewhat distorted by factors including noise contamination and cardiac motion artifacts. The DW data set comprised breath-hold DW images, which are preferred to respiratory-triggered images for lesion identification. Different pulse triggering may mitigate artifacts caused by cardiac motion. ADC may also vary based on hardware, human, and biological variables. Even when utilizing a similar MR system, ADC values may vary since SS EPI is susceptible to low intrinsic SNR and numerous distortions. Few researchers have examined the repeatability of ADC in the liver parenchyma (26,27).

5.1. Conclusion

The results of our study showed that there is a significant overlap between the ADC values of various benign or malignant lesions at both sequences, DWI showed to be useful in characterizing localized hepatic lesions yet must

always be utilized in combination with standard MRI. It appears appropriate to combine DWI with conventional imaging techniques. We expect that by using DWI instead of dynamic MRI, we will learn enough about the characteristics of malignant and benign liver lesions to reduce the frequency of biopsies, risks, and costs.

Ethical approval

Ethical approval was obtained from the Tehran University of Medical Sciences Ethics Committee (Cod number: IR.TUMS.SPH.REC.1396.2297)

Consent for publication

Not applicable`

Availability of data and materials

The datasets used and analyzed during the current study are available from the corresponding author on reasonable request

Competing interests

The authors declare that they have no competing interests

Authors' contributions

H.J.T and H.N.S.A contributed to study concept and design; R.A.B, A.D.A, and H.A.D collected the data; A.M.E and H.A.D carried out analysis and interpretation of data; H.J.T and H.N.S.A performed drafting of the manuscript; All authors read and approved the final manuscript.

ACKNOWLEDGMENTS

This article has been derived from a Ph.D.

thesis at Tehran University of Medical Sciences. We would like to thank the cooperation of all the research centers and units.

REFERENCES

1. Parikh T, Drew SJ, Lee VS, Wong S, Hecht EM, Babb JS, et al. Focal liver lesion detection and characterization with diffusion-weighted MR imaging: comparison with standard breath-hold T2-weighted imaging. *Radiology*. 2008 , 246(3), 812-22.
2. Hussain SM, Zondervan PE, IJzermans JN, Schalm SW, de Man RA, et al . Benign versus malignant hepatic nodules: MR imaging findings with pathologic correlation. *Radiographics*. 2002, 22(5), 1023-36.
3. Taouli B, & Koh DM. Diffusion-weighted MR imaging of the liver. *Radiology*. 2010, 254(1), 47.
4. Alonso-Torres A, Fernández-Cuadrado J, Pinilla I, Parrón M, de Vicente E, et al. Multidetector CT in the evaluation of potential living donors for liver transplantation. *Radiographics*. 2005, 25(4), 1017-30.
5. Robinson P J, & Ward J. *MRI of the Liver: A Practical Guide*. CRC Press,2016.
6. Vergara ML, Fernández M, & Pereira R. Diffusion-weighted MRI characterization of solid liver lesions. *Revista Chilena De Radiología*. 2010, 16(1), 510.
7. Kim T, Murakami T, Takahashi S, Hori M, Tsuda K, & Nakamura H. Diffusion-weighted single-shot echoplanar MR imaging for liver disease. *AJR. American journal of roentgenology*. 1999, 173(2), 393-8.
8. Feuerlein S, Pauls S, Juchems MS, Stuber T, Hoffmann MH, Brambs HJ, et al. Pitfalls in abdominal diffusion-weighted imaging: how predictive is restricted water diffusion for malignancy. *American Journal of Roentgenology*. 2009, 193(4), 1070-16.
9. Ichikawa T, Haradome H, Hachiya J, Nitatori T, & Araki T. Diffusion-weighted MR imaging with a single-shot echoplanar sequence: detection and characterization of focal hepatic lesions. *AJR. American journal of roentgenology*. 1998, 170(2), 397-402.

10. Silva AC, Evans JM, McCullough AE, Jatoi MA, Vargas HE, & Hara AK. MR imaging of hypervascular liver masses: a review of current techniques. *Radiographics*. 2009, 29(2), 385-402.
11. Bozgeyik Z, Onur MR, & Poyraz AK. The role of diffusion weighted magnetic resonance imaging in oncologic settings. *Quantitative imaging in medicine and surgery*. 2013, 3(5), 269.
12. Goshima S, Kanematsu M, Kondo H, Yokoyama R, Kajita K, Tsuge Y, et al. Diffusion-weighted imaging of the liver: optimizing b value for the detection and characterization of benign and malignant hepatic lesions. *Journal of Magnetic Resonance Imaging: An Official Journal of the International Society for Magnetic Resonance in Medicine*. 2008, 28(3), 691-7.
13. Ba-Ssalamah A, Qayyum A, Bastati N, Fakhrai N, Herold CJ, & Caseiro Alves F. P4 radiology of hepatobiliary diseases with gadoxetic acid-enhanced MRI as a biomarker. *Expert review of gastroenterology & hepatology*. 2014, 8(2), 147-60.
14. Kilickesmez O, Bayramoglu S, Inci E, & Cimilli T. Value of apparent diffusion coefficient measurement for discrimination of focal benign and malignant hepatic masses. *Journal of medical imaging and radiation oncology*. 2009, 53(1), 50-5.
15. Crocetti D, Palmieri A, Pedullà G, Pasta V, D'Orazi V, & Grazi GL. Peliosis hepatis: Personal experience and literature review. *World Journal of Gastroenterology*. 2015, 21(46), 13188.
16. Nasu K, Kuroki Y, Tsukamoto T, Nakajima H, Mori K, & Minami M. Diffusion-weighted imaging of surgically resected hepatocellular carcinoma: imaging characteristics and relationship among signal intensity, apparent diffusion coefficient, and histopathologic grade. *American Journal of Roentgenology*. 2009, 193(2), 438-44.
17. Chung YE, Kim MJ, Park YN, Choi JY, Pyo JY, Kim YC, et al. Varying appearances of cholangiocarcinoma: radiologic-pathologic correlation. *Radiographics*. 2009, 29(3), 683-700.
18. Mehrabi A, Kashfi A, Fonouni H, Schemmer P, Schmied BM, Hallscheidt P, et al. Primary malignant hepatic epithelioid hemangioendothelioma: a comprehensive review of the literature with emphasis on the surgical therapy. *Cancer: Interdisciplinary International Journal of the American Cancer Society*. 2006, 107(9), 2108-21.
19. Soyer P, Corno L, Boudiaf M, Aout M, Sirol M, Placé V, et al. Differentiation between cavernous hemangiomas and untreated malignant neoplasms of the liver with free-breathing diffusion-weighted MR imaging: comparison with T2-weighted fast spin-echo MR imaging. *European journal of radiology*. 2011, 80(2), 316-24.
20. ZADEH, Firoozeh Abolhasani, et al. Cytotoxicity evaluation of environmentally friendly synthesis Copper/Zinc bimetallic nanoparticles on MCF-7 cancer cells. *Rendiconti Lincei. Scienze Fisiche e Naturali*, 2022, 1-7.
21. ROHMAH, Martina Kurnia, et al. Modulatory role of dietary curcumin and resveratrol on growth performance, serum immunity responses, mucus enzymes activity, antioxidant capacity and serum and mucus biochemicals in the common carp, *Cyprinus carpio* exposed to abamectin. *Fish & Shellfish Immunology*, 2022, 129: 221-230.
22. ARIF, Anam, et al. The functions and molecular mechanisms of Tribbles homolog 3 (TRIB3) implicated in the pathophysiology of cancer. *International Immunopharmacology*, 2023, 114: 109581.
23. MARGIANA, Ria, et al. Functions and therapeutic interventions of non-coding RNAs associated with TLR signaling pathway in atherosclerosis. *Cellular Signalling*, 2022, 100: 110471.

24. H. A. Al-Hchaimi, M. F. Alhamaidah, H. Alkhfaji, M. T. Qasim, A. H. Al-Nussairi and H. S. Abd-Alzahra, "Intraoperative Fluid Management for Major Neurosurgery: Narrative study," 2022 International Symposium on Multidisciplinary Studies and Innovative Technologies (ISMSIT), 2022, pp. 311-314, doi: 10.1109/ISMSIT56059.2022.9932659.
25. MOHAMMED, Zainab; QASIM, Maytham T. The Relationship between Insulin Resistance and Hypertension in Patient with Hypertensive. HIV Nursing, 2022, 22.2: 1659–1663-1659–1663.
26. LEI, Zimeng, et al. Detection of abemaciclib, an anti-breast cancer agent, using a new electrochemical DNA biosensor. *Frontiers in Chemistry*, 2022, 10.
27. BASHAR, Bashar S., et al. Application of novel Fe₃O₄/Zn-metal organic framework magnetic nanostructures as an antimicrobial agent and magnetic nanocatalyst in the synthesis of heterocyclic compounds. *Frontiers in Chemistry*, 2022, 10.